Supporting Information

S1 DFT calculation details

All the spin-polarized hybrid HSE 06 calculations were performed with Perdew-Burke-Ernzerhof (PBE) functional using the VASP code[1-3]. The project-augmented wave (PAW) approach was used to represent the core-valence electron interaction with electrons from Ti 3*p*, 3*d*, 4*s*; O 2*s*, 2*p*; and H 1*s* shells explicitly included in the calculations. The valence electronic states were expanded in plane wave basis sets with energy cutoff of 450 eV, and the occupancy of the one-electron states was calculated using the Gaussian smearing with SIGMA = 0.05 eV. Geometric structures were relaxed using the BFGS minimization scheme until the Hellman-Feynman forces on each ion were less than 0.05 eV/Å. The HSE 06 optimized lattice parameters of the bulk rutile TiO_2 are a=4.572, b=4.572, c=2.954 Å, being well consistent with the experimental data (a=4.594, b=4.594, c=2.959 Å). The density of state (DOS) analyses were also performed. As shown in Fig. S1, a 3.12 eV bandgap was calculated, which agrees well with the experimental value (~3.05 eV). Therefore, both the geometry optimization and the electronic description are all well consistent with experimental results, thus ensuring our calculation accuracy.

The rutile (110) surface was modeled by a four-Ti-layer $p(1\times4)$ periodical slab supercell with a ~15Å vacuum between slabs, and a corresponding $2\times1\times1$ k-points mesh was used during optimizations. All the atoms were allowed to relax on the purpose of avoiding up-shift of occupied states of the oxygens in the fixed layer with lower electrostatic potentials. In order to compare HSE 06 functional with DFT+U, we also performed the DFT+U calculations with U terms applied to O 2p state, and a large U value (U(*p*) = 6.3 eV)[4] was used. In the calculation of the oxygen vacancy formation energies (E_{vf}) of lattice O_{br}^{2-} and O_{br}^{-} radical, the U terms were applied to both Ti 3d (U(*d*) = 4.2 eV)[4,5] and O 2p (U(*p*) = 6.3 eV) states, respectively, because of the formation of Ti^{3+} ions (the electron is localized on Ti^{4+}) when removing an oxygen.

S2 Description of added OH for various radicals

For the negatively charged species O_{br}^{2-}, O_{3c}^{2-}, O_{sub}^{2-} (corresponding to Figure 3a, 3c and 3d, respectively), there is one OH added on the bottom layer in each case in the

calculations, in order to trap an electron for each species to form O_{br}^-, O_{3c}^- and O_{sub}^- radicals (see also Figure S4a, S4c and S4d). With respect to the $\cdot OH_t$ radical (Figure 3e), there is no additional OH added on the bottom layer, as shown in Figure S4e and the reason is the following: (i) when an OH group adsorbs on the surface, it usually exists as an electron acceptor in the form of OH^-, resulting in a hole in the system; (ii) the hole can diffuse to the adsorbed OH^- and oxidize it forming ·OH radical. Therefore, to model ·OH radical, no additional OH on the bottom layer is needed. However, for the case of $\cdot OH_{br}$ (Figure 3b), two additional OH groups are added on the bottom layer (see Figure S4b) with the following consideration: (i) one OH is added with the purpose of removing the extra electron introduced by the H atom, forming an OH^- and a protonated bridge oxygen (OH_{br}^-); (ii) the other one is introduced to trap an electron to form the $\cdot OH_{br}$ radical. It should be noted that in the calculation of the HTC of $\cdot OH_{br}$, the bulk hole reference state is localized at the same bulk oxygen as that in other cases.

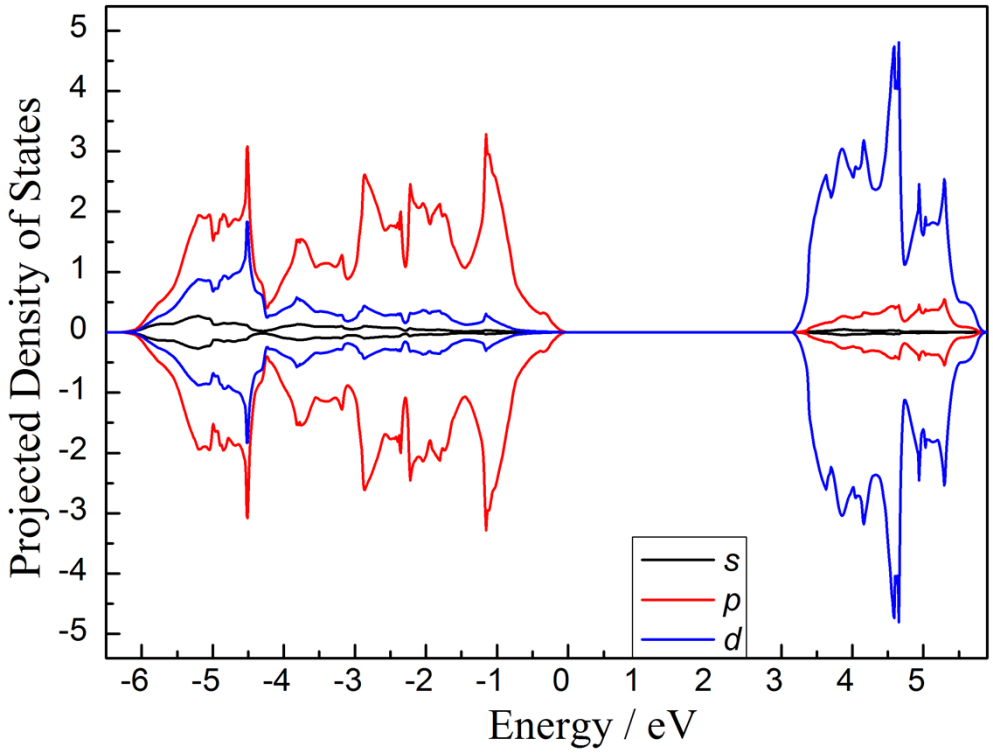

Figure S1 The calculated PDOS of bulk rutile TiO_2 using HSE 06 functional. All the states below 0 are occupied.

S3 DOS analysis of surface adsorbed CH_3O^* species

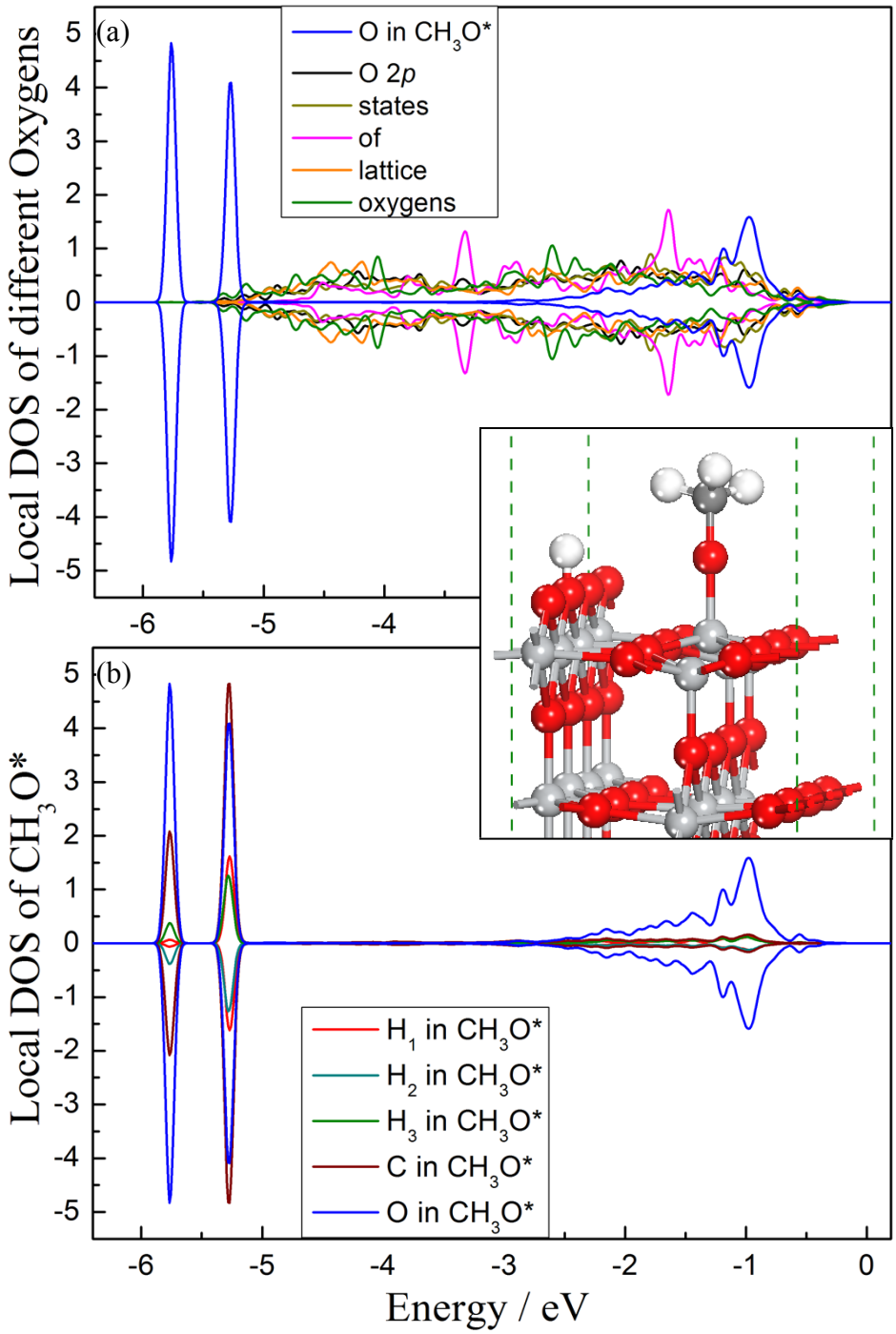

Figure S2 Local DOSs of different oxygen atoms (**a**), containing both lattice oxygen atoms and the one in CH_3O^*, and the adsorbed CH_3O^* (**b**) on a terminal Ti^{4+} using HSE 06 functional. The optimized geometry structure of dissociative methanol is illustrated in the insert.

S4 Derivation of H_2O/O_2 potential

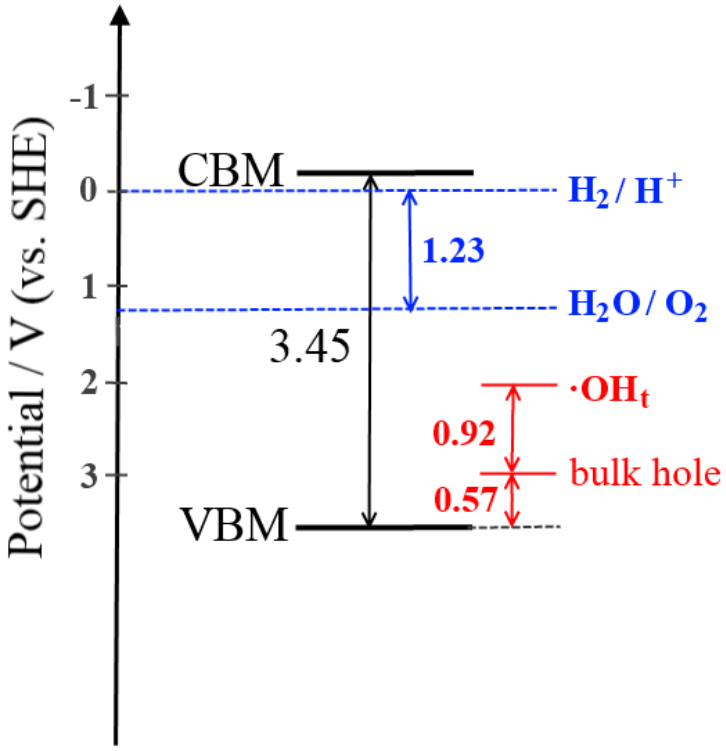

Figure S3 The energy levels of both VBM and CBM of rutile TiO_2(110), as well as the potentials of $H^+ + e^- \rightarrow 1/2\ H_2$ and $O_2 + 4H^+ + 4e^- \rightarrow 2H_2O$. The calculated energy level of $\cdot OH_t$ radical is also shown. The oxidative potential of bulk hole was reported as 0.57 V (*vs*. VBM) by Cheng et al.[6]

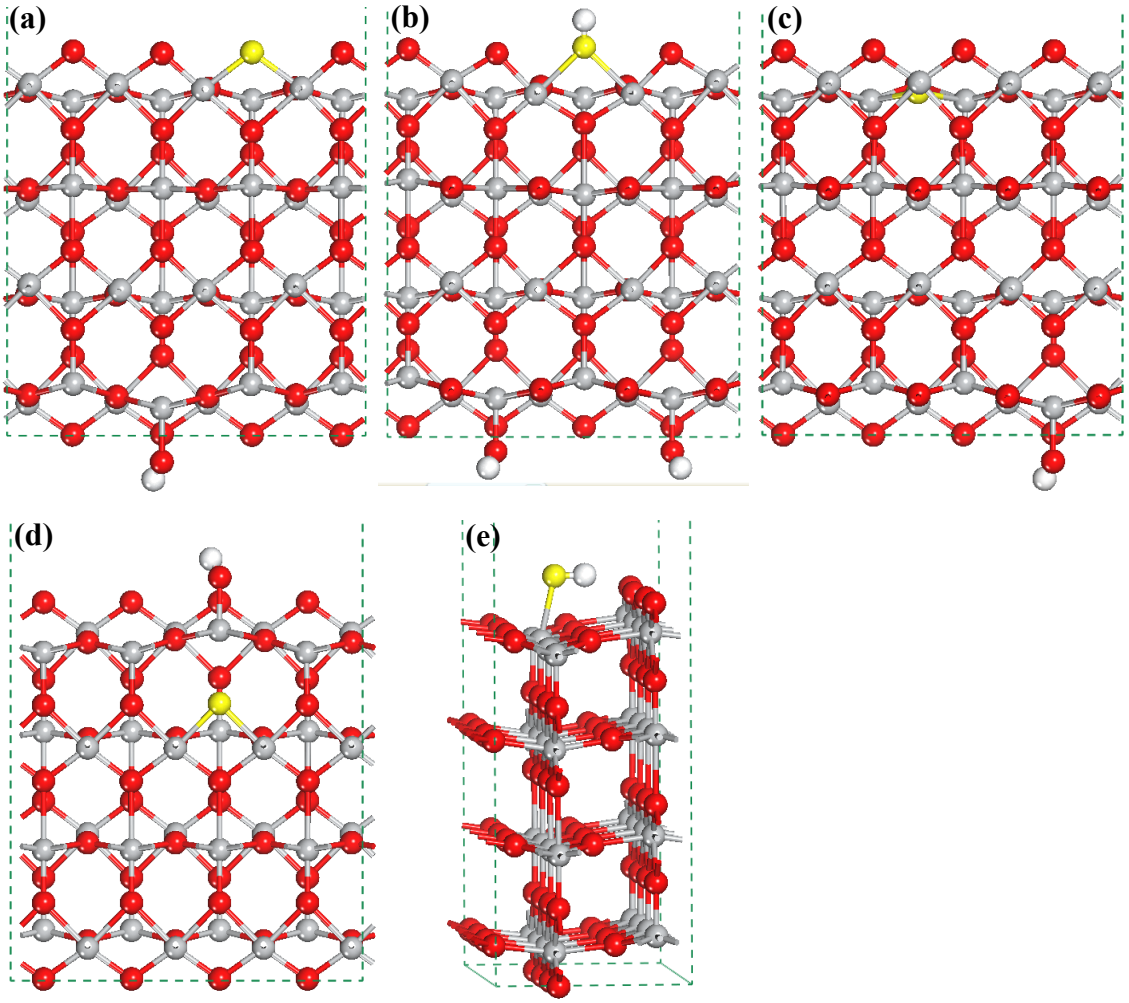
(a)
(b)
(c)
(d)
(e)

Figure S4 Side views of structures of various spin-polarized radicals for O_{br}^- (a), $\cdot OH_{br}$ (b), O_{3c}^- (c), O_{sub}^- (d) and $\cdot OH_t$ (e) from HSE 06. The oxygen atoms in radicals are highlighted in yellow.

References:

1 A. Janotti, J. B. Varley, P. Rinke, N. Umezawa, G. Kresse, C. G. Van de Walle, *Phys. Rev. B,* 2010, **81**, 085212.
2 G. Kresse, J. Hafner, *Phys. Rev. B*, 1994, **49**, 14251;
3 G. Kresse, J. Furthmuller, *Comput. Mater. Sci.*, 1996, **6**, 15.
4 Y. F. Ji, B. Wang, Y. Luo, *J. Phys. Chem. C*, 2012, **116**, 7863.
5 X. Ma, Y. Dai, M. Guo, B. Huang, *langmuir,* 2013, **29**, 13647-13654
6 J. Cheng, M. Sulpizi, J. VandeVondele, M. Sprik, *ChemCatChem*, 2012, **4**, 636.